Nexus of Future Materials
https://nfmjournal.com/

Radiation Shielding Analysis of Barium-Titanium-Borate Glasses Doped with Zinc Oxide

E. L. Ruiz

Department of Physics, University of Pennsylvania, Philadelphia, United States

Keywords:

radiation shielding
glasses
borate glasses
heavy metal oxides
Phy-X software

Abstract

The radiation shielding properties of a barium-zin-titanium-borate glass system were theoretically reported. Four glasses were investigated, with compositions of (80-x) B_2O_3-10BaO-10TiO_2-xZnO, (x = 20, 25, 30 and 35 mol%), and densities of 3.593, 3.751, 3.908, and 4.066 g/cm^3, respectively. The Phy-X software was used to determine the radiation shielding parameters for these samples, using energies from Cs-137, Co-60, and Na-22. The mass attenuation coefficient, half value layer, and mean free path of the glasses were studied. The MAC value found that the higher the ZnO content in the samples, or the higher the density of the glasses, the greater the MAC value no matter the energy. The LAC value evaluated the relationship between LAC and density and resulted in materials with higher densities having higher LAC values at all energies. The HVLs of the glasses found that the higher the ZnO concentration, or the lower the borate content, in the materials, the lower the HVLs, and thus the thinner the shield needs to be to attenuate the same level of photons. The TVL ratio between the glasses with the lowest and highest ZnO content remained above one, which means that samples with higher ZnO content had lower TVL values than samples with lower ZnO content. The MFP values found that the higher the density of the glasses, the lower the MFP values. Therefore, the higher the ZnO content in this glass system, the more desirable the shielding material.

1. Introduction

The field of radiation shielding relies on fabricating, experimenting, and improving upon materials that are used to block radiation. Much research has been conducted on the harmful effects that radiation can have on the human body and the environment. Such ionizing radiation, however, is essential for many applications, and thus safety precautions must be taken to ensure the safety of all that come near the source of radiation.

Developments in the field of medicine have led to life saving technologies such as radiation therapy and X-ray imaging, both of which require the patient to be close to the source of radiation. The radiation shielding materials are then placed to absorb the radiation between the patient and the ionizing particles, as well as to contain the scattered photons [1-4].

* Corresponding author:
E-mail address: e.lacommeeastchester@gmail.com

Received 7 June 2024; Accepted 2 August 2024;
Published 12 August 2024
https://doi.org/10.70128/584050

The conditions of the application must be considered when developing a shielding material, as certain materials are better applied to specific applications. For example, concrete is used to line the walls of rooms or structures that contain radiation, such as rooms with X-ray machines or the walls in a nuclear reactor. Concrete is a low-cost material that is structurally very reliable to build walls and other such structures, which makes it ideal for this application. It suffers from water loss and crack development over time, but recent developments for self-healing concrete have improved such drawbacks. Lead is also often used as a radiation shield, most often used as a lead apron to protect patients from X rays. But because of its toxic nature, alternatives are used instead such as bismuth oxide [5-7].

Radiation shielding glasses are formed by mixing metal oxides together in varying concentrations. Depending on the metal oxides used, the characteristics of the glasses change. The first step in creating a glass system is deciding on the glass former, which is the metal oxide that forms the backbone of the glass network [8-12]. Borate, or B2O3, is a common choice for a glass former. Borate forms trigonal units that are altered to tetrahedral structures as other metal oxides are added into the glass. Alkali metals and alkaline earth metals act as glass modifiers, which alter the glass network but do not form part of the backbone. Barium oxide, or BaO, and zinc oxide, ZnO act as such glass modifiers. The third type of metal oxide is a glass intermediate, which can either be a glass modifier or a glass former, depending on the composition of the glass system. Metal oxides such as TiO2 are glass intermediates [13-17].

In this study, a glass system with a composition of (80-x) B2O3-10BaO-10TiO2-xZnO, x = 20, 25, 30 and 35 mol%. Several parameters were determined and analyzed to gain a comprehensive understanding of the shielding abilities of the glasses.

2. Materials and methods

The glasses in this work were prepared using the melt quenching method. The glass composition is given in Table 1.

Table 1. The chemical composition of the investigated glasses.

Glass code	B_2O_3	TiO_2	BaO	ZnO	Density (g/cm^3)
S1	60	10	10	20	3.593
S2	55	10	10	25	3.751
S3	50	10	10	30	3.908
S4	45	10	10	35	4.066

The mass attenuation coefficient (MAC) describes how much a material can attenuate a beam of radiation that passes through it, and is a general mechanism for determining the effectiveness of a material to block radiation. The MAC value of a material is determined using $\frac{\mu}{\rho}$, where μ is the linear attenuation coefficient, and ρ is the density of the material. The linear attenuation coefficient, or LAC, measures how much a material can attenuate radiation, but instead considers the density of the material within the parameter. The LAC of a material can be calculated using $\mathrm{In}\frac{I}{I_0}/x$, where I_0 is the initial density of the radiation before it enters the material, I is the radiation intensity after through the material, and x is the material's thickness. The half-value layer of a material, or HVL, is a measure of the thickness of a material needed to reduce the intensity of radiation to half of its original value, and is a practical measure to understand the effectiveness of a material to attenuate radiation. HVL can be measured using the formula: $HVL = \frac{\ln(2)}{\mu}$, where μis again the LAC of the material. TVL stands for the tenth-value layer of a material and measures the thickness of a material required to reduce the intensity of a radiation beam to one-tenth of its initial value. Similar to HVL, TVL has a formula of TVL $= \frac{\ln(10)}{\mu}$. Lastly, the MFP or mean free path refers to the average

passes through a material before interacting with photons within the sample. Its formula can be calculated through MFP $=\frac{1}{\mu}$, suggesting an inverse relationship with LAC of the material. In this work, we used Phy-X software to study the radiation shielding parameters for the investigated glasses [19].

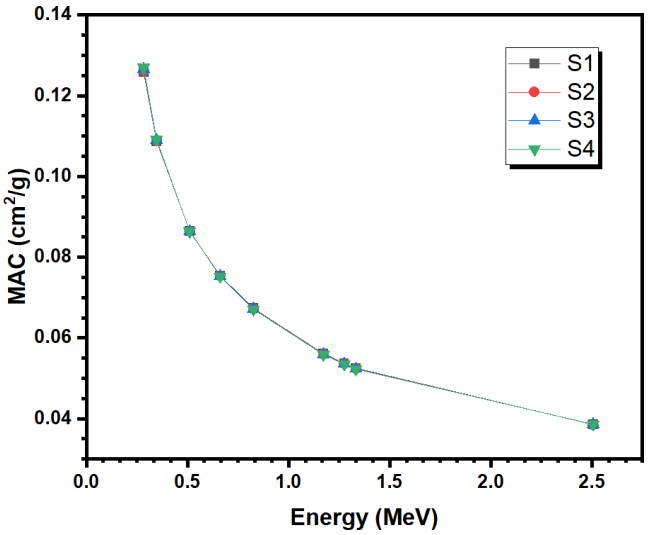

Fig. 1. The mass attenuation coefficient for the prepared glasses

Fig.1 highlights the MAC of the investigated glasses as a function of energy [20]. The MAC of the prepared glasses are close together at all energies, with the S4 sample having the highest MAC and the S1 glass having the lowest. For example, at 0.347 MeV, the MAC values are equal to 0.1087, 0.1089, 0.1089, and 0.1092 cm^2/g for S1, S2, S3, and S4, respectively. At 1.333 MeV, meanwhile, the MAC values are equal to 0.0525, 0.0524, 0.0524, and 0.0523 cm^2/g for the same respective glasses. Therefore, the higher the ZnO concentration in the materials, and the lower the B_2O_3 content, the greater the MAC values. Thus, the S4 sample has the highest MAC value at all energies. Additionally, the MAC values of all four glasses decrease as the energy of the photons increases. For instance, the MAC value of the S1 sample is equal to 0.126, 0.086, 0.067, 0.054, and 0.039 cm^2/g at 0.284, 0.511, 0.826, 1.275, and 2.506 MeV. For the S4 sample, meanwhile, the MAC values for the same respective energies are equal to 0.127, 0.086, 0.067, 0.054, and 0.039 cm^2/g.

It should be noted that all the MAC values for the S4 sample are lower than the S1's MACs, although at higher energies the values are within 0.001 cm^2/g from each other.

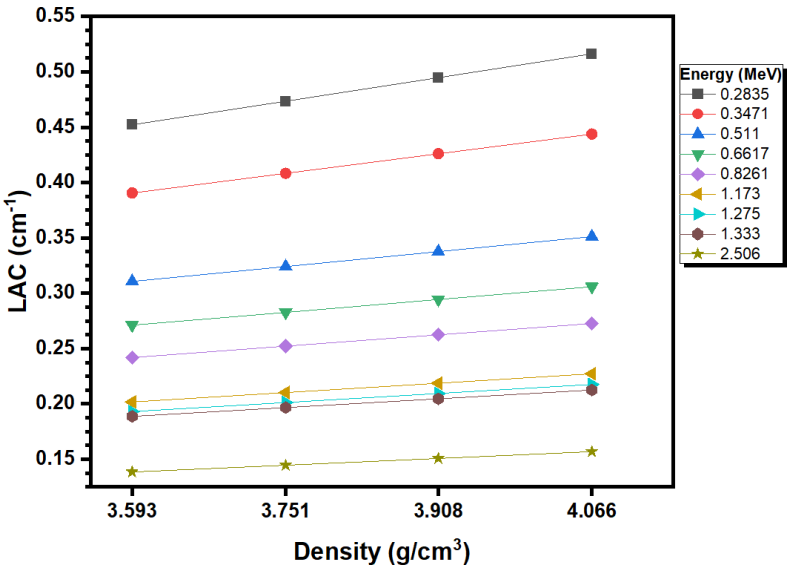

Fig. 2. The linear attenuation coefficient (cm^{-1}) vs the density

Fig.2 demonstrates the LAC values of the investigated samples as a function of density. As the energy of the radiation increases, the LAC values decrease [21-23]. For instance, at a density of 3.751 g/cm^3, the LAC values are equal to 0.474, 0.324, 0.252, 0.201, and 0.145 cm^{-1} at 0.284, 0.511, 0.826, 1.275, and 2.506 MeV. Meanwhile, at 4.066 g/cm^3, the LAC values are equal to 0.516, 0.351, 0.273, 0.218, and 0.157 at the same respective energies. The density in the figure shows that having a higher density leads to a greater LAC. For instance, at 0.662 MeV, the LAC values are equal to 0.271 cm^{-1} at 3.593 g/cm^3, 0.283 cm^{-1} at 3.751 g/cm^3, 0.294 cm^{-1} at 3.908 g/cm^3, and 0.306 cm^{-1} at 4.066 g/cm^3. Because of this trend, the glasses with the greatest ZnO content, which in this case is S4, has the highest LAC value, and is more desirable than the other investigated samples.

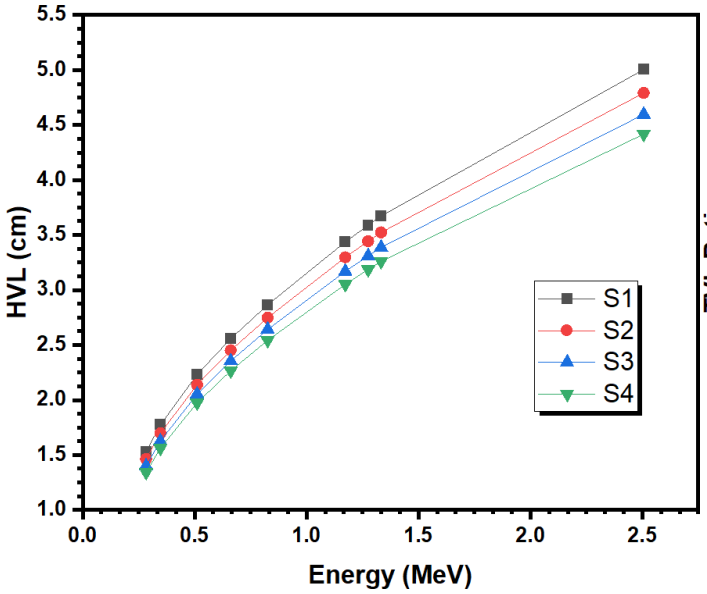

Fig. 3. The half value layer for the prepared glasses.

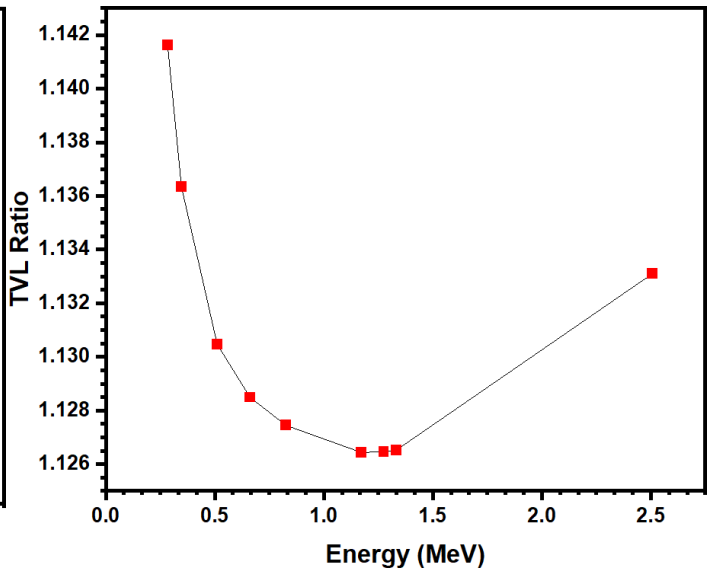

Fig. 4. The ratio between the TVL of the S1 and S4 sample at a different range of energies.

Fig. 3 highlights the HVL of the prepared glasses against increasing energy at the selected energy range. The HVL values can be observed to increase, from 1.342-1.533 cm at 0.284 MeV to 4.417-5.005 cm at 2.506 MeV. Specifically, the HVL values of the S2 sample are equal to 1.464, 2.138, 2.748, 3.443, and 4.792 cm at 0.284, 0.551, 0.826, 1.275, and 2.506 MeV. The HVL values of the S3 sample at the same respective energies are equal to 1.401, 2.053, 2.631, 3.310, and 4.598 cm. Thus, this upward trend shows that thicker shields are needed to stop radiation with higher energy, while photons of smaller energy require a thinner sample. The figure also shows that the S1 sample has the largest HVL value, followed by the S2 glass, S3 glass, and lastly the S4 glass with the smallest. For instance, at 0.347 MeV, the HVL values are equal to 1.775 cm for the S1 glass, 1.697 for the S2 glass, 1.627 cm for the S3 sample, and 1.562 cm for the S4 glass. At 1.333 MeV, meanwhile, the HVL values are equal to 3.673, 3.524, 3.387, and 3.260 cm for the same respective samples. Thus, for any radiation energy, a thicker glass is needed for the S1 sample to attenuate the same number of photons as the other materials, with the least thickness needed for the S4 glass.

Fig. 4 explores the ratio between the TVL of the S1 and S4 sample at a wide range of energies. The ratio starts out at its highest at 0.284 MeV, being equal to 1.1416. The ratio begins to drop as the radiation energy increases to the middle energy range, to 1.1363 cm at 0.347 MeV, and 1.1274 cm at 0.826 MeV. At higher energies, the ratio increases, to 1.1265 at 1.333 MeV and 1.1331 at 2.506 MeV. The up and down trend of the ratio describes the difference between the TVL value as the radiation energy changes. At lower and very high energies, the difference between the TVL of the S1 and S4 samples is highest, while in the middle energy range this difference decreases. However, because the ratio remains above one at all energies, the TVL of the S1 sample is greater than the TVL of the S4 glass across all energies.

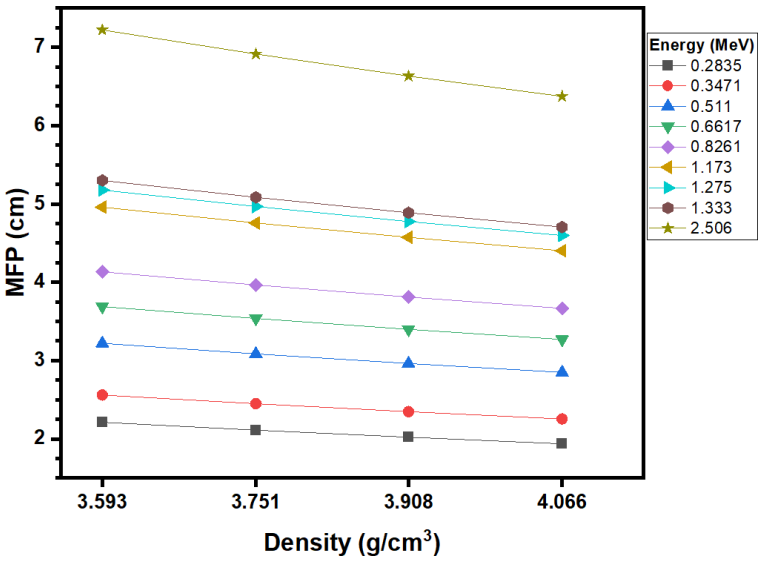

Fig. 5. The mean free path as a function of the density.

Fig. 5 demonstrates the MFP of the glasses against density. The MFP of the glasses decreases as the density of the glasses increases. For example, at 0.511 MeV, the MFP values are equal to 3.219, 3.085, 2.962, and 2.848 cm at 3.595, 3.751, 3.908, and 4.066 g/cm^3, respectively. At 1.333 MeV, meanwhile, the MFP values are equal to 5.299, 5.083, 4.887, and 4.704 cm for the same respective densities. Therefore, adding more ZnO to the samples, which leads to an increase in density, lowers the MFP of the glasses, which often leads to a more effective shield. The figure also shows that the MFP of the glasses increases as the radiation energy increases at all densities. For example, at 3.595 g/cm^3, the MFP values are equal to 2.211, 3.689, 4.958, and 7.221 cm at 0.284, 0.662, 1.173, and 2.506 MeV, respectively, while at a density of 4.066 g/cm^3, the MFPs are respectively equal to 1.937, 3.269, 4.402, and 6.373 cm. Therefore, the higher the radiation energy, the greater the distance between subsequent collisions no matter the density of the samples.

2. Conclusion

A glass system consisting of borate, titanium oxide, barium oxide, and zinc oxide in varying concentrations was theoretically analyzed in this study. The Phy-X software was used to determine various radiation shielding parameters for these materials. The MAC values had an inverse trend with energy, with the highest MAC values occurring at the lowest tested energy, decreasing until the higher energy range. The LAC values highlighted that having a higher density led to a greater LAC, such as at 0.662 MeV, the LAC values are equal to 0.271 cm^{-1} at 3.593 g/cm3, 0.324 cm^{-1} at 3.751 g/cm^3, 0.338 cm^{-1} at 3.908 g/cm^3, and 0.306 cm^{-1} at 4.066 g/cm^3. The HVL values showed that at all energies, they followed the order of S1 > S2 > S3 > S4. The ratio between the TVL of the S1 and S4 sample starts out at 1.1416 at 0.284 MeV, dropping to 1.1274 at 0.826 MeV, and then rising to 1.1331 at 2.506 MeV. The MFP of the glasses were investigated against their density, finding that the MFO of the glasses increases as the radiation energy increases at all densities. Thus, the S4 sample, which has the highest ZnO content, has the most desirable shielding properties at all energies.

References

[1] Gaurav Tyagi, Anupam Singhal, Srikanta Routroy, Dipendu Bhunia, Mukund Lahoti, A review on sustainable utilization of industrial wastes in radiation shielding concrete, Materials Today: Proceedings 32 (2020) 746–751.

[2] Hualiang Liu, Jianjun Shi, Huiqiong Qu, Dexin Ding, an investigation on physical, mechanical, leaching and radiation shielding behaviors of barite concrete containing recycled cathode ray tube funnel glass aggregate, Construction and Building Materials 201 (2019) 818–827.

[3] Nastasia Saca, Lidia Radu, Viorel Fugaru, Maria Gheorghe, Ionela Petre, Composite materials with primary lead slag content: Application in gamma radiation shielding and waste encapsulation fields, Journal of Cleaner Production 179 (2018) 255-265.

[4] A. Zughbi, M.H. Kharita, A.M. Shehada, determining optical and radiation characteristics of cathode ray tubes' glass to be reused as radiation shielding glass, Radiation Physics and Chemistry 136 (2017) 71–74.

[5] Mira Natasha Azman, Nadin Jamal Abualroos, Khatijah Aisha Yaacob, Rafidah Zainon, Feasibility of nanomaterial tungsten carbide as lead-free nanomaterial-based radiation shielding, Radiation Physics and Chemistry 202 (2023) 110492.

[6] P. Sopapan, J. Laopaiboon, O. Jaiboon, C. Yenchai, R. Laopaiboon, Feasibility study of ecycled CRT glass on elastic and radiation shielding properties used as x-ray and gamma-ray shielding materials, Progress in Nuclear Energy 119 (2020) 103149.

[7] Yoon Suk Choi, Seon Min Lee, Fundamental properties and radioactivity shielding performance of concrete recycled cathode ray tube waste glasses and electric arc furnace slag as aggregates, Progress in Nuclear Energy 133 (2021) 103649.

[8] Varsha Agrawal, Rini Paulose, Rahul Arya, Gaurav Rajak, Abhishek Giri, Abhijit Bijanu, Sunil K. Sanghi, Deepti Mishra, Prasanth N, Anup Kumar Khare, Varsha Parmar, Mohammed Akram Khan, Abhay Bhisikar, Avanish Kumar Srivastava, Shabi Thankaraj Salammal, Green conversion of hazardous red mud into diagnostic X-ray shielding tiles, Journal of Hazardous Materials 424 (2022) 127507.

[9] Abdelmoneim Saleh, Comparative shielding features for X/Gamma-rays, fast and thermal neutrons of some gadolinium silicoborate glasses, Progress in Nuclear Energy 154 (2022) 104482.

[10] A. Saleh, Rizk Mostafa Shalaby, Nermin Ali Abdelhakim, comprehensive study on structure, mechanical and nuclear shielding properties of lead free Sn–Zn–Bi alloys as a powerful radiation and neutron shielding material, Radiation Physics and Chemistry 195 (2022) 110065.

[11] Abdelmoneim Saleh, M. G. El-Feky, M. S. Hafiz, N. A. Kawady, Experimental and theoretical investigation on physical, structure and protection features of TeO2-B2O3 glass doped with PbO in terms of gamma, neutron, proton and alpha particles, Radiation physics and chemistry 202 (2022) 110586.

[12] A. Shahboub, G. El Damrawi, A. Saleh, a new focus on the role of iron oxide in enhancing the structure and shielding properties of Ag2O–P2O5 glasses, Eur. Phys. J. Plus (2021) 136:947.

[13] A. Shahboub, A. Saleh, A. K. Hassan, G. El Damrawi, EPR studies and radiation shielding properties of silver aluminum phosphate glasses, Applied Physics A (2023) 129:410.

[14] M. Adib, N. Habib, I. Bashter, A. Saleh, Neutron transmission through pyrolytic graphite crystal II, Annals of Nuclear Energy 38 (2011) 802–807

[15] M. Adib, N. Habib, I. Bashter, H.N. Morcos, M. Fathallah, M.S. El-Mesiry, A. Saleh, Neutron characteristics of single-crystal magnesium fluoride, Annals of Nuclear Energy 60 (2013) 163–171 Con,

[16] W. Chaiphaksa, P. Borisut, N. Chanthima, J. Kaewkhao, N.W. Sanwaranatee, Mathematical calculation of gamma ray's interaction in bismuth gadolinium silicate glass using WinXCom program, Materials Today: Proceedings 65 (2022) 2412-2415,

[17] Reza Bagheri, Alireza Khorrami Moghaddam, and Hassan Yousefnia, Gamma Ray Shielding Study of Barium-Bismuth-Borosilicate Glasses as Transparent Shielding Materials using MCNP-4C Code, XCOM Program, and Available Experimental Data, Nuclear Engineering and Technology 49 (2017) 216-223.

[18] A. Acikgoz, G. Demircan, D. Yılmaz, B. Aktas, S. Yalcin, N. Yorulmaz, Structural, mechanical, radiation shielding properties and albedo parameters of alumina borate glasses: Role of CeO2 and Er2O3, Mater. Sci. Eng.: B 276 (2022), 115519.

[19] Erdem Şakar, Özgür Fırat Özpolat, Bünyamin Alım, M.I. Sayyed, Murat Kurudirek, Phy-X / PSD: Development of a user friendly online software for calculation of parameters relevant to radiation shielding and dosimetry, Radiation Physics and Chemistry 166 (2020) 108496.

[20] H. Karami, V. Zanganeh, M. Ahmadi, Study nuclear radiation shielding, mechanical and Acoustical properties of TeO2-Na2O-BaO-TiO2 alloyed glasses, Progress in Radiation Physics and Chemistry 208 (2023) 110917.

[21] R. Rajaramakrishna, W. Chaiphaksa, S. Kaewjaeng, S. Kothan, J. Kaewkhao, Study of radiation shielding and luminescence properties of 1.5 μm emission from Er3+ doped zinc yttrium borate glasses, Progress in Optik - International Journal for Light and Electron Optics 289 (2023) 171273.

[22] Bulent Aktas, Abuzer Acikgoz, Demet Yilmaz, Serife Yalcin, Kaan Dogru, Nuri Yorulmaz, The role of TeO2 insertion on the radiation shielding, structural and physical properties of borosilicate glasses, Progress in Journal of Nuclear Materials 563 (2022) 153619.

[23] Bilgehan Guven, Ediz Ercenk, Senol Yilmaz, Investigation of radiation shielding properties of basalt-based glasses: Binodal/Spinodal decomposition effect theory, Progress in Nuclear Energy 163 (2023) 104810.